

Charge transfer, lattice distortion, and quantum confinement effects in Pd, Cu, and Pd–Cu nanoparticles; size and alloying induced modifications in binding energy

Saurabh K. Sengar,¹ B. R. Mehta,^{1,a)} and Govind Gupta²

¹*Thin Film Laboratory, Department of Physics, Indian Institute of Technology Delhi, New Delhi 110016, India*

²*Surface Physics Group, National Physical Laboratory (CSIR), New Delhi 110012, India*

(Received 8 February 2011; accepted 19 April 2011; published online 13 May 2011)

In this letter, effect of size and alloying on the core and valence band shifts of Pd, Cu, and Pd–Cu alloy nanoparticles has been studied. It has been shown that the sign and magnitude of the binding energy shifts is determined by the contributions of different effects; with quantum confinement and lattice distortion effects overlapping for size induced shifts in case of core levels and lattice distortion and charge transfer effects overlapping for alloying induced shifts at smaller sizes. These results are important for understanding gas molecule-solid surface interaction in metal and alloy nanoparticles in terms of valence band positions. © 2011 American Institute of Physics.

[doi:10.1063/1.3590272]

Alloying and nanoparticle route are two important methodologies employed for modifying the structural and electronic properties of Pd and consequently improving the Pd–H interaction for enhanced catalytic properties.¹ Pd nanoparticles have shown improved Pd–H interaction and higher catalytic properties, due to size-dependent shift of Pd 4d centroid and increased surface area.² Core-shell Pd-alloy nanoparticles have shown suitable catalytic properties for oxygen reduction because of the lowering of d-band centroid.³ A study of the changes in the core and valence electron binding energy (BE) is crucial for understanding the role of metal addition or reduction in size on the Pd–H interaction. In general, the variation in BE of core levels and valence bands in Pd and Pd-thin film and bulk alloys has been explained in terms of initial state and final state effects.^{4,5} In spite of its direct relevance in important technologies such as hydrogen sensing and storage, there are only limited reports on variation in core and valence levels in Pd and Pd-alloy nanoparticles.^{4,6} The effect of size on valence and core levels in case of Pd, Pd-alloy islands and nanoparticulate thin films grown by vacuum evaporation technique was studied by controlling the thickness and coverage of the polycrystalline islands.^{4,6} In the present letter, metal and alloy nanoparticles have been prepared by gas phase synthesis followed by in-flight sintering to reduce the chemical ligand and polycrystallinity induced effects. Structural and electronic properties of Pd–Cu alloy nanoparticles of different sizes have been studied and compared with those of Pd and Cu nanoparticles of similar sizes prepared under identical conditions.

Gas phase synthesis setup consisting of (i) an aerosol generator (GFG1000, PALAS GmbH, Germany) for forming Pd–Cu agglomerates, (ii) a UV charger for charging the agglomerates, (iii) sintering furnace for changing the primary nanoagglomerates into compact spherical and monocrystalline nanoparticles via in-flight sintering, and (iv) an electrostatic precipitator to deposit charged nanoparticles onto substrates

was used to synthesize Pd–Cu alloy nanoparticles. In the spark generator primary alloy nanoparticles, which become agglomerates by coagulation are produced by a discharge between the electrodes of Pd and Cu (99.95% pure) whose separation is automatically adjusted to be 2 mm by a step motor during the deposition. In order to obtain crystalline spherical nanoparticles these agglomerates are in-flight sintered at 700 °C. The crystalline, spherical Pd–Cu particles with well-defined sizes formed in gas phase were deposited directly onto the Si substrates and carbon coated Cu transmission grids. Glancing angle x-ray diffraction (GAXRD) and x-ray photoelectron microscopy (XPS) measurements were performed using X'Pert, PRO-PW 3040 and Model 1257, Perkin Elmer, USA equipments. Valence and core level spectra of these samples were obtained using Al K α radiation as the excitation source after 10 min. Ar ion cleaning, BE values were referenced using the C 1s peak position at 284.6 eV.

It is observed from the high resolution transmission electron microscopy (HRTEM) images (Fig. 1) that both the unsintered and sintered nanoparticles are crystalline with an average size of 3.5 nm (PdCu3.5 sample) and 20 nm (PdCu20 sample), respectively. Pd and Cu nanoparticles (Pd3.5, Cu3.5, Pd20, and Cu20 samples) were prepared under identical conditions and have similar average sizes. GAXRD studies reveal the face centered cubic structure of Pd and Cu nanoparticles and a lattice contraction (LC) of 0.2% for Pd and 0.9% for Cu with decrease in size. A similar LC has been reported in Pd metal nanoparticles with decrease in size.⁴ This observed XRD shift has been attributed to surface bond contraction with coordination number reduction and enhanced surface area at lower particle size.⁴ In case of Pd–Cu nanoparticles, (111) peak is observed to lie between the peaks of Pd and Cu nanoparticles (of same size), which confirms the Pd–Cu alloy formation. Energy dispersive x-ray analysis (EDX) studies carried out on Pd–Cu3.5 sample sintered at different temperatures ranging from 300 to 900 °C has confirmed that the average atomic composition during compaction is 65:35 (Pd:Cu) and remains unchanged and thus the change in the XRD peak positions is not due to any composition change. Pd–Cu nanoparticles show a lattice

^{a)}Author to whom correspondence should be addressed. Electronic mail: brmehta@physics.iitd.ac.in.

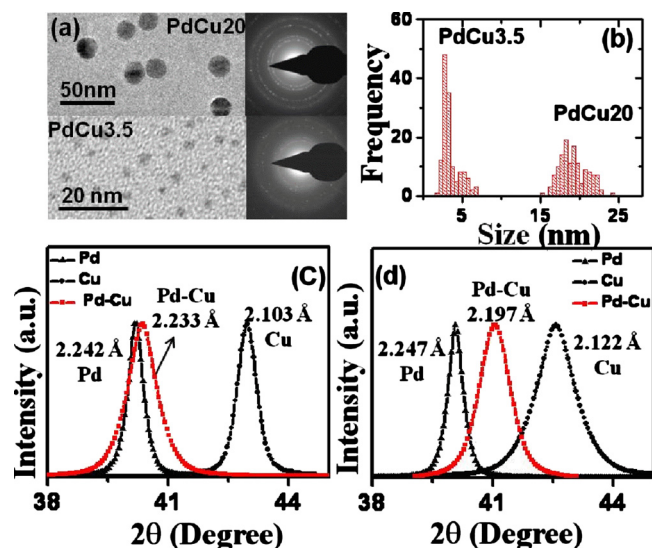


FIG. 1. (Color online) (a) high-resolution TEM images of the PdCu_{3.5} (bottom) and PdCu₂₀ (top) samples along with their (b) histograms, showing size distributions of PdCu_{3.5} and PdCu₂₀ nanoparticle samples. GAXRD spectra, showing (111) peaks of Pd, Cu, and Pd–Cu nanoparticles having (c) 3.5 nm size and (d) 20 nm size. Corresponding d-values are also given.

expansion (LE) of 1.6% on reduction in size. LE in nanoparticles may be due to the stress field of the vacancies and vacancy clusters in the grain boundaries resulting from the increased volume energy because of increased interface energy and surface tension.⁷

XPS core-level (Pd 3d_{5/2} and Cu 2p_{3/2}) and valence band spectra (Pd 4d and Cu 3d bands) of Pd, Cu, and Pd–Cu nanoparticles are shown in Fig. 2. Based on the XPS results, changes in the peak positions due to reduction in size from 20 to 3.5 nm (ΔE_s) for Pd, Cu, and Pd–Cu nanoparticles are given in Table I. In case of Pd and Cu metal nanoparticles, Pd 3d_{5/2} and Cu 2p_{3/2} peaks show +ve ΔE_s of 0.16 eV and 0.88 eV, respectively, whereas, in Pd–Cu alloy nanoparticles, Cu 2p_{3/2} and Pd 3d_{5/2} peaks show a –ve ΔE_s of 0.19 eV and 0.52 eV, respectively. Pd 4d and Cu 3d valence band peaks of metal and alloy nanoparticles follow the same trend in ΔE_s as observed in core levels but with a relatively smaller magnitude for metals and larger magnitude for alloys. The observed shift in core and valence band peaks can be explained on the basis of the combined effect of lattice distortion (LD) and quantum confinement (QC). It has been shown that LD alters the chemical bonding, which in turn leads to changes in the core and valence band BEs.⁸ LC results in increased BEs while LE results in decreased BEs. Due to quantum or space confinement, electron energy levels shift toward higher energy on reduction in the width of the confining potential. Loosely bound valence electrons are expected to be less affected by the QC effect in comparison to core levels.⁴ The observed positive ΔE_s in Pd 3d_{5/2} and Cu 2p_{3/2} peaks in case of metal nanoparticles is due to the overlap of two +ve effects of QC and LC. The larger ΔE_s for Cu 2p_{3/2} peak in comparison to Pd 3d_{5/2} peak is due to larger LC observed in case of Cu nanoparticles, as revealed by XRD results. In case of Pd–Cu nanoparticles, the effect of LE is opposite to the +ve effect due to QC. The negative values of ΔE_s of Cu 2p_{3/2} and Pd 3d_{5/2} peaks in Pd–Cu alloy shows that LE effect dominates over the QC effect. In case of Pd and Cu nanoparticles, positive values of ΔE_s in

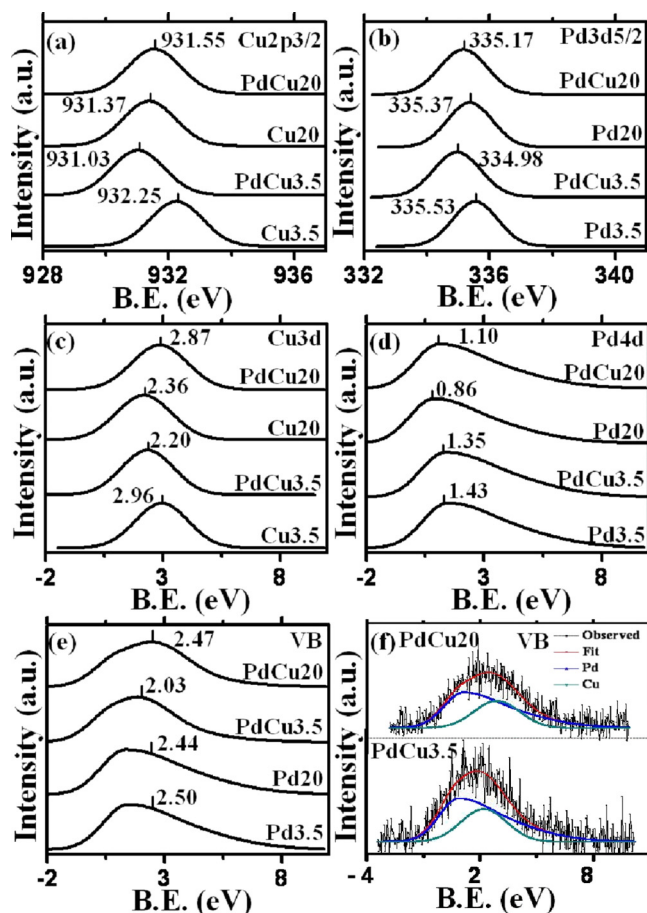


FIG. 2. (Color online) Core level (a) Cu 2p_{3/2}, (b) Pd 3d_{5/2} and valence band, (c) Cu 3d, (d) Pd 4d spectra in Pd, Cu, and Pd–Cu nanoparticle samples. (e) Comparison of valence bands of Pd_{3.5} and Pd₂₀ samples with the modified valence bands of PdCu_{3.5} and PdCu₂₀ nanoparticle samples and (f) the deconvolution of valence bands into two separate Pd 4d and Cu 3d bands in PdCu_{3.5} and PdCu₂₀ nm samples.

Cu 3p and Pd 4d are lower in comparison to corresponding core levels (Cu 2p_{3/2} and Pd 3d_{5/2}) as the positive contribution due to QC effect is reduced. Due to the same reason, negative values of ΔE_s for Cu 3p and Pd 4d in Pd–Cu alloy nanoparticles are larger in magnitude.

The shift in the peak positions on alloying (ΔE_a) in case of 20 and 3.5 nm particles with respect to the corresponding values for Pd and Cu nanoparticles of similar sizes are given in Table II. In case of 20 nm Pd–Cu alloy nanoparticles, ΔE_a is –ve for both Pd 3d_{5/2} and Pd 4d bands and +ve for Cu 2p_{3/2} and Cu 3d peaks. It is also observed that ΔE_a val-

TABLE I. XPS core level and valence band peak shifts (ΔE_s) due to reduction in size from 20 to 3.5 nm. LC: lattice contraction, LE: lattice expansion, QC: quantum confinement.

Peak	Metal/alloy	ΔE_s (eV)	Proposed explanation
Pd 3d _{5/2}	Pd	(+)0.16	+LC, +QC
Cu 2p _{3/2}	Cu	(+)0.88	+LC, +QC
Pd 3d _{5/2}	Pd–Cu	(–)0.19	–LE, +QC
Cu 2p _{3/2}	Pd–Cu	(–)0.52	–LE, +QC
Pd 4d	Pd	(+)0.06	+LC
Cu 3d	Cu	(+)0.60	+LC
Pd 4d	Pd–Cu	(–)0.24	–LE
Cu 3d	Pd–Cu	(–)0.67	–LE

TABLE II. XPS core level and valence band peak shifts (ΔE_a) in Pd–Cu nanoparticles due to alloying effect. CT: charge transfer.

Peak	Size (nm)	ΔE_a (eV)	Proposed explanation
Pd $3d_{5/2}$	20	(–)0.20	–CT
Pd $4d$	20	(–)0.32	–CT
Cu $2p_{3/2}$	20	(+)0.18	+CT
Cu $3d$	20	(+)0.51	+CT
Pd $3d_{5/2}$	3.5	(–)0.55	–CT, –LE
Pd $4d$	3.5	(–)0.62	–CT, –LE
Cu $2p_{3/2}$	3.5	(–)1.22	+CT, –LE
Cu $3d$	3.5	(–)0.76	+CT, –LE

ues are large for valence levels in comparison to core levels. For 3.5 nm Pd–Cu nanoparticles, ΔE_a values are –ve for Pd and Cu core and valence bands. Because of the charge transfer (CT) resulting from the electronegativity differences, BE values of the constituent elements shift in the opposite direction. Pd is more electronegative (2.2) than Cu (1.9), which results in the charge flow from Cu to Pd on alloying and hence the BE of Cu increases while that of Pd decreases. Since CT affects valence levels more, hence ΔE_a values are large in magnitude for valence levels in comparison to core levels for 20 nm nanoparticle size, as shown in the Table II. In case of 3.5 nm Pd–Cu nanoparticles, negative values of ΔE_a for both the core levels (Pd $3d_{5/2}$ and Cu $2p_{3/2}$) and valence band peaks (Pd $4d$ and Cu $3d$) can be explained in terms of the combined effect of CT due to alloying and LE due to reduction in size from 20 to 3.5 nm. It may also be mentioned that LE effect dominates over the CT effect in case of 3.5 nm alloy nanoparticles. Also the effect of LE is more dominant in Cu $2p_{3/2}$ and Cu $3d$ peaks, which is consistent with the XRD results.

A detailed density function theory has shown that the position of d-band centroid with respect to Fermi energy is the most important parameter determining the reactivity of metal surface and determines the shift of the bonding and antibonding states formed during interaction, degree of filling of the antibonding states, and magnitude of the coupling matrix.⁹ Results of the present letter show that the position of the Pd $4d$ centroid in Pd nanoparticles is strongly affected due to size induced lattice contraction and the QC effects are minimal. The positive shift in the position of the valence band on reduction in size from 20 to 3.5 nm indicates size induced enhancement in the reactivity of Pd nanoparticles. Larger magnitude of the hydrogen induced optical changes in Pd–Gd based switchable mirrors has been explained in terms of the shift of the Pd $4d$ centroid away from Fermi energy on size reduction.¹⁰ Observations of increased oxidation of formic acid and shift of Pd $4d$ band on reduction in nanoparticle size has been reported in Pd nanoparticles.¹¹ In-

creased water-gas shift reactivity observed in case of Cu nanoparticles in comparison to Cu foils is also consistent with the above results.¹² In case of Pd–Cu nanoparticles, the size induced shift in the valence band centroid is negative due to LE effects and thus the reactivity of Pd–Cu nanoparticles is expected to be higher at larger sizes. Pd–Cu bilayer thin films have been shown to exhibit lower surface reactivity in comparison to Pd thin films.¹³

The results of the present letter provide a clear understanding of the effect of size and alloying on the electronic properties of Pd alloy nanoparticles. It is shown that BE shifts of core and valence band electrons in Pd, Cu, and Pd–Cu alloy nanoparticles is determined by the relative sign and magnitude of the overlapping effects of LD, CT, and QC, which may be inferred from the physics underlying these effects. Overlap of LD and QC determine the relative magnitude of BE shifts due to size reduction. Similarly, CT and LD determine the peak shifts due to alloying. The size induced shift in the valence band position observed in Cu, Pd, and Cu–Pd nanoparticles is largely due to LE or LC effects and is consistent with the experimental results of increased reactivity in Pd and Cu and decreased surface reactivity in Pd–Cu bilayer thin films. It is expected that the results of the present letter will be helpful in modifying Pd–H interaction in Pd alloy nanoparticles by controlling the nanoparticle size, composition and constituent metal (Cu, Ag, or Ni).

One of the authors Saurabh K Sengar is thankful to Council of Scientific and Industrial Research, India for providing junior research fellowship. The financial support of project sponsored by Nanomission program of DST, India is also acknowledged.

¹M. Khanuja, S. Kala, B. R. Mehta, and F. E. Kruijs, *Nanotechnology* **20**, 015502 (2009).

²I. Aruna, B. R. Mehta, and L. K. Malhotra, *Appl. Phys. Lett.* **87**, 103101 (2005).

³W. Tang and G. Henkelman, *J. Chem. Phys.* **130**, 194504 (2009).

⁴I. Aruna, B. R. Mehta, L. K. Malhotra, and S. M. Shivaprasad, *J. Appl. Phys.* **104**, 064308 (2008).

⁵W. Olovsson, I. A. Abrikosov, and B. Johansson, *J. Electron Spectrosc. Relat. Phenom.* **127**, 65 (2002).

⁶K. R. Harikumar, S. Ghosh, and C. N. R. Rao, *J. Phys. Chem. A* **101**, 536 (1997).

⁷W. Qin, Z. H. Chen, P. Y. Huang, and Y. H. Zhuang, *J. Alloys Compd.* **292**, 230 (1999).

⁸B. Richter, H. Kuhlbeck, H. J. Freund, and P. S. Bagus, *Phys. Rev. Lett.* **93**, 026805 (2004).

⁹B. Hammer and J. K. Norskov, *Nature (London)* **376**, 238 (1995).

¹⁰I. Aruna, B. R. Mehta, L. K. Malhotra, and S. M. Shivaprasad, *Adv. Funct. Mater.* **15**, 131 (2005).

¹¹W. P. Zhou, A. Lewera, R. Larsen, R. I. Masel, P. S. Bagus, and A. Wieckowski, *J. Phys. Chem. B* **110**, 13393 (2006).

¹²J. A. Rodriguez, P. Liu, X. Wang, W. Wen, J. Hanson, J. Hrbek, M. Pérez, and J. Evans, *Catal. Today* **143**, 45 (2009).

¹³M. Khanuja, B. R. Mehta, and S. M. Shivaprasad, *J. Chem. Sci.* **120**, 573 (2008).